DE GRUYTER OPEN

Mathematical Modelling in Civil Engineering
Vol. 11-No. 1 : 20-28 – 2015
Doi: 10.1515/mmce-2015-0003

A THREE-DIMENSIONAL ANALYSIS OF THE WHEEL - RAILWAY CONTACT IN CASE OF A CHARGE TRANSFER

CRISTINA TUDORACHE - Assistant Ph.D., Railway Vehicles Engineering Department, University Politehnica of Bucharest, Romania, cristi_tudorache2003@yahoo.com
IOAN SEBEŞAN - Ph.D. Professor, Railway Vehicles Engineering Department, University Politehnica of Bucharest, Romania, ioan_sebesan@yahoo.com

Abstract: A series of factors are acting are acting on the wheels of the railway vehicle causing load transfers capable of having an effect on safety transportation The evaluation of vehicle – runway interaction phenomena establishes traffic safety conditions. In this paper we present a three-dimensional approach of the wheel - railway contact in case of load transfer and for a path with shortfall or with profile S78 super-elevation excess. The vehicle – runway interaction phenomena establishes traffic safety conditions. In this paper we present a three-dimensional approach of the wheel - railway contact in case of load transfer and for a path with shortfall or with profile S78 super-elevation excess is analyzed.

Keywords: contact ellipse, sliding/adherence area, contact forces, safety against derailment.

1. Introduction

Over the years there have been a number of theories developed on the wheel-railway contact in order to resolve the problems relate to the interaction with the railway track and to improve the dynamic performances of vehicles.

One of those who laid the foundations of the theory of rolling friction was Carter [1], who used a two-dimensional model that assimilates the wheel with a cylinder and the railway with a board. The bodies found in direct contact are elastically deformable and between them only longitudinal sliding occurs. Later on, Johnson and Vermeulen [2], extended the two-dimensional theory developed by Carter for arbitrary half-spaces. According to these the contact surface between the two bodies engaged in a rotary movement is divided into a bonding zone called stick and a sliding one called slip. Also, the stick zone has an elliptic form being arranged tangential to the inside of contact ellipse.

Halling, Haines and Ollerton, [3], developed approximately the same theory regarding the elliptic contact with longitudinal pseudo-sliding. The contact area was divided in a series of strips displayed parallel with the rolling direction and then each band was studied by expanding Carter's two-dimensional theory.

In the end, starting from the hypothesis of his predecessors, Kalker, [4] laid the foundations of an exact three-dimensional analysis of the contact with friction. He takes into account, for each of the points within the contact area, the local sliding speeds and the local distortions of the bodies found in contact. The relations established by Kalker are valid though only for the small pseudo-sliding movement, being used in studies regarding the stability of moving vehicles.

Kalker's merit, [5], consists in the fact that he introduced the effect of spinning movement and invalidated Lévi's isotropy principle [6]. The value of the friction index is strongly influenced by the shape of the rolling profiles and by the load carried on the wheel. On the other hand, the linear relations established by Kalker are valid only for the small pseudo-sliding movements, being used in studies carried out for establishing the stability of moving vehicles.

The stability of a vehicle is influenced also by the load transfers caused by quasi-static and dynamic forces generated primarily by the unevenness of the railway. The position of the normal load shifts during rolling. A shift of the load over the first rolling wheel of the leading axle implies an increase in the stability limit in derailment imposed by the safety against derailment [7].

The literature from this field presents numerous criteria for assessing the safety against derailment; criteria, which take into account, the ratio between the forces displayed vertically and tangentially. Among these, Nadal's formula [8], Weinstock's [9] limit criterion and the limitation of the contact area on the wheel [10, 11, 12] are noticeable.

The present paper proposes a three-dimensional approach of the contact between the wheel and the railway in the case of a shift in load. The analysis is done by using the CONTACT software, which assimilates the contact area through half-space units and divides it through the method of the end element. In the contact area the theory of linear elasticity is applied. CONTACT establishes the shape and size of the contact area between the elastically deformable bodies found in tangential contact (normal loads). This is achievable only if the shape of the profiles from the contact point is known.

Consequently, after this short presentation of the current state of the rolling contact analysis we will present in sections no. 2 and 3 aspects of the load transferring ratio and the tangential contact conditions. Section no. 4 is dedicated to an example of numerical analysis for a contact between a wheel having the S78 profile and a UIC 60 1:20 railway showing a roll with shortfall and super-elevation excess, while in the very end section the main aspects of the present study will be presented.

2. Load transfers on the vehicle axles

The forces from the interaction area created between the wheel and the railway are in balance with the exterior forces that are transmitted to the axles in the form of linking forces (fig.1):

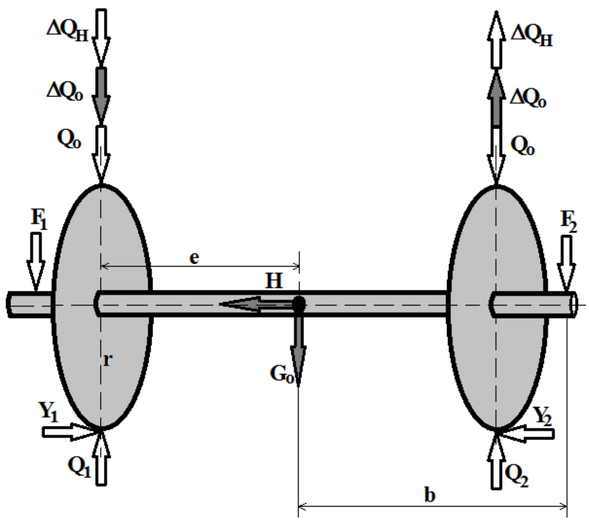

Fig.1 - Forces transmitted to the vehicle's axle

At the level of each axle mounted wheel load Q_0 acts which originates from the gravitational forces. If the axle rolls on a smooth railway, without super-elevation, then the total load $2Q_0$ is uniformly spread on the two wheels. But, due to the unevenness of the railway and of the quasi-static or dynamic forces, transfers of load take place during the rolling on the wheels, which lead to a disequilibrium of the contact forces.

The transfer of load on the axle represents the half-difference between the loads applied on the two wheels, i.e.:

$$\Delta Q = \frac{Q_1 - Q_2}{2} \tag{1}$$

Where Q_1 – the load on the first wheel, Q_2 – load on the second wheel. If we relate to the transfer the load ΔQ, then the loads on the two wheels are given by the following equations:

$$\begin{aligned} Q_1 &= Q_o + \Delta Q \\ Q_2 &= Q_o - \Delta Q \end{aligned} \tag{2}$$

The factors that produce load transfers on the axle are of various origins. The external forces represent one of these factors as they are transmitted through the springs of the vertical suspension of the wheel that are also containing the vertical resistance of the dampers caused by the torsion of the railway. Thus, the load transfer caused by these forces, noted as F_1 and F_2, is given by the following equation:

$$\Delta Q_o = \frac{1}{2}\frac{(F_1 - F_2)b}{e} \tag{3}$$

The equation (3) is valid if the following condition is respected:

$$Q_1 + Q_2 = F_1 + F_2 + G_o = 2Q_o$$

where G_0 is the weight of the axle.

Another factor is the transversal force called H, or chassis leading force, which appears in the axle hub and is transmitted to the vehicle chassis though the axle bed. This force contains inertia forces caused by shifts in the vehicle direction as well as the opposing forces appeared in its rotation. The transversal force creates a turning point of the axle acting above the contact area between the wheel and the railway track and is also creating a transfer of load

$$\Delta Q_H = \frac{Hr}{2e} \tag{4}$$

If the load transfers ΔQ_0 and ΔQ_H are taken into consideration, then the load on each wheel will be:

$$\begin{aligned} Q_1 &= Q_o + \Delta Q_o + \Delta Q_H \\ Q_2 &= Q_o - \Delta Q_o - \Delta Q_H \end{aligned} \tag{5}$$

and the equilibrium condition $Q_1 + Q_2 = 2Q_0$ will be achieved.

According to the ORE B-55 Committee, the maximum accepted shifts of load in quasi-static conditions and on a twisted railway must not exceed $\Delta Q_0 / Q_0 \le 0{,}6$ (where $\Delta Q_0 / Q_0$ is defined as transfer coefficient) for a flank angle of the wheel edge angle of 700 and for a situation where the H transversal force is almost equal to 0. This situation is applied for vehicles fitted with steerable axles. The limit of the load transfers on axles is established according to the criteria regarding safety against derailment.

When talking about the scenario regarding the unload of the first rolling wheel while going over a curve at low speed, a maximum super-elevation and a high twist of the railway result:

- if the rolling is done with super-elevation excess: $Q_1 = Q_o - \Delta Q_o - \Delta Q_H$
- if the rolling is done with super-elevation deficiency: $Q_1 = Q_o + \Delta Q_o + \Delta Q_H$

With the same value of the transfer coefficient the $\Delta Q_0 / Q_0$, $(Y_1 / Q_0)_{lim}$ is reduced at the same ratio as the wheel radius; with smaller wheels the derailment coefficient is higher. On the other hand, increasing the flank maximum angle of the wheel edge is favorable for increasing the safety against derailment as it increases both the minimum and the maximum guiding capacity of the axle.

3. The issue regarding the tangential contact

The analysis of the wheel-railway tangential contact consists in determining the distribution of the traction force, namely the contact pressures and relative sliding speeds in relation to the dimensions of the contact area [13, 14]. The distribution of pressure within the contact area, if Hertz's hypotheses are respected, is done following an elliptic paraboloid, as described in the equation [7, 15]:

$$p(x,y) = p_o\sqrt{1-\left(\frac{x}{a}\right)^2-\left(\frac{y}{b}\right)^2} \tag{6}$$

where p_0 represents the maximum pressure developed in the center of the contact ellipse, a and b represent the semi-axes of the contact ellipse.

The normal load, Q_0, applied on the wheel in relation to the normal pressure is given by the following equation:

$$Q_o = \int\int p dxdy \tag{7}$$

If p from equation (6) is replaced in equation (7) and the integration is achieved then we can obtain

$$Q_o = \frac{2}{3} p_o \pi ab \tag{8}$$

Thus the relation (7) becomes:

$$p(x,y) = \frac{3}{2\cdot\pi\cdot a\cdot b} Q_o\sqrt{1-\left(\frac{x}{a}\right)^2-\left(\frac{y}{b}\right)^2} \tag{9}$$

The a and b semi-axes, as well as their alignment along or transversally to the railway track, are determined according to the following equation:

$$a = m\left(3\pi Q_o\frac{k_1+k_2}{4(A+B)}\right)^{1/3}, \quad b = n\left(3\pi Q_o\frac{k_1+k_2}{4(A+B)}\right)^{1/3} \tag{10}$$

where m and n are coefficients determined by Hertz in conjunction to $\cos\tau = (A-B)/(A+B)$, $A = 1/r$, $B = 1/\rho_r + 1/\rho_s$, r – wheel rolling radius, ρ_r, ρ_s – wheel buckling radius in the contact point, $k_{1,2}$ – a constant which depends of the nature of the material from which the two bodies found in contact are made of, $k_{1,2} = \left(1-\vartheta_{1,2}^2\right)/\pi E_{1,2}$, $\upsilon_{1,2}$ – Poisson's coefficient, $E_{1,2}$ – longitudinal elasticity module.

Kalker's leaner theory represents an approach, at a higher level, of the tangential contact. Thus, assuming that for small pseudo-sliding values the sliding area is very small, the theory asserts that the whole contact surface is assimilated to an adherence area. Consequently the condition to the limit is given by the following equations:

- Within the contact ellipse:

$$0 = \mathrm{w}_{\mathrm{x,y}} = \mathrm{V}\cdot\left(\nu_{\mathrm{x}} - \varphi\cdot y,\ \nu_{\mathrm{y}} + \varphi\cdot x\right) - V\frac{\partial u(x,y)}{\partial x} \tag{11}$$

- Outside the contact ellipse:

$$0 = \mathrm{p(x,y)} \tag{12}$$

Through the integration of the (11) equation we obtain

$$g(y) = \text{-}\mathrm{V}\cdot\mathrm{u(x,y)} + V\left(\nu_x x - \varphi\cdot x\cdot y,\ \nu_y x - \frac{1}{2}\varphi\cdot x^2\right) \tag{13}$$

where g(y) is an arbitrary function.

The g(y) arbitrary function is determined by the condition where the traction has to be continuous at the limit of the driving direction of the traction surface, where the railway and the wheel are in direct contact. The result thus obtained does not comply with the limit value for the friction force at the rear limit of the contact surface [16]. The traction increases up to the rear limit of the contact area, then the normal load is removed and the traction is suddenly dropping to zero. Because of this, the friction coefficient value has a discontinuous evolution up to infinite. The calculus of the g(y) function leads to a linear expression of the dependence between the forces and pseudo-sliding:

$$\begin{aligned} F_x &= -a \cdot b \cdot G \cdot C_{11} \cdot \nu_x \\ F_y &= -a \cdot b \cdot G\left(C_{22} \cdot \nu_y + \sqrt{a \cdot b} \cdot C_{23} \cdot \varphi\right) \\ M_\varphi &= -\left(\sqrt[3]{a \cdot b} \cdot G \cdot C_{32} + (a \cdot b)^2 G \cdot C_{33} \cdot \varphi\right) \end{aligned} \tag{14}$$

where: a, b – contact ellipse semi-axes, ν_x, ν_y, φ - longitudinal, transversal and spinning pseudo-sliding movements in the contact points, C_{11} , C_{22}, $C_{23,32}$, C_{33} – Kalker's coefficients which depend on the values of Poisson's coefficient and are determined according to the equations displayed below [16]:

$$\begin{aligned} &C_{11} = -\frac{\partial F_x}{\partial \nu_x} / (a \cdot b \cdot G), \quad C_{22} = -\frac{\partial F_y}{\partial \nu_y} / (a \cdot b \cdot G) \\ &C_{23} = -\frac{\partial F_y}{\partial \varphi} / \left(\sqrt[3]{a \cdot b} \cdot G\right)_{\nu_x = \nu_y = \varphi = 0} \end{aligned} \tag{15}$$

Kalker is also defining the pseudo-sliding coefficients as following:

$$\kappa_x = \frac{a \cdot b \cdot G \cdot C_{11} \cdot \nu_x}{\mu \cdot N}, \quad \kappa_y = \frac{a \cdot b \cdot G \cdot C_{22} \cdot \nu_y}{\mu \cdot N}, \quad \kappa_\varphi = \frac{\sqrt[3]{a \cdot b} \cdot G \cdot C23 \cdot \varphi}{\mu \cdot N} \tag{16}$$

The longitudinal, transversal and spinning pseudo-sliding movements are determined based on the following relations:

$$\nu_x = \frac{w_x}{V}, \quad \nu_y = \frac{w_y}{V}, \quad \varphi = \frac{r \cdot \omega_s}{V}, \tag{17}$$

ω_s - the spinning angular speed. The $w_{x,y}$ pseudo-sliding speeds are established according to relation (1) and their spatial orientation for a rolling axle is shown in fig. 2.

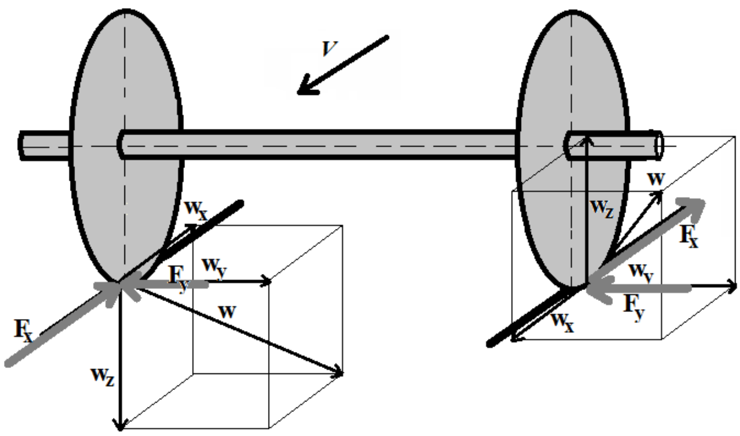

Fig.2 - Spatial orientation of the sliding speeds from the wheel-railway couple.

4. Numerical application

In the following lines we will present the behavior of an axle fitted with S78 wheels (the nominal rolling radius is 460 mm) while rolling over a UIC 60, 1:20 railway, with excess and deficiency on super-elevation (nominal deficiency I = 70 mm, super-elevation excess E = -I).

The behavior at the level of the contact points is analyzed three-dimensionally. The rolling speed of the axle is 35m/s. The normal load on the wheel is considered to be 100kN and the load transfer is 60kN.

For a more accurate analysis of the contact area between the wheel and the railway track, from the beginning the profile of the rolling surfaces as well as the contact points between the two parties was established. The profiles were established by using the method of circular sectors and the contact points were established through the method of the minimum distance. The contact points were analyzed for a given headway of 6mm in comparison to the initial position.

First, the influence of the load shift over the size and shape of the sliding and adherence zones belonging to the first rolling wheel is analyzed for the scenario with the travelling over a railway with excess and then with deficiency on super-elevation.

Thus, in figure 3, it can easily be observed that in both situations the distribution of the sliding areas is in accordance with the strips theory, that is, with the behavior of the null pseudo-sliding [17]. Moreover, the influence of load transfer over the size of the contact point and of the adherence area can be observed. one can also notice that when rolling over the portions of the track that have super-elevation deficiency the contact area is excessively reduced in the case of a load transfer while the sliding area along the rail is extended.

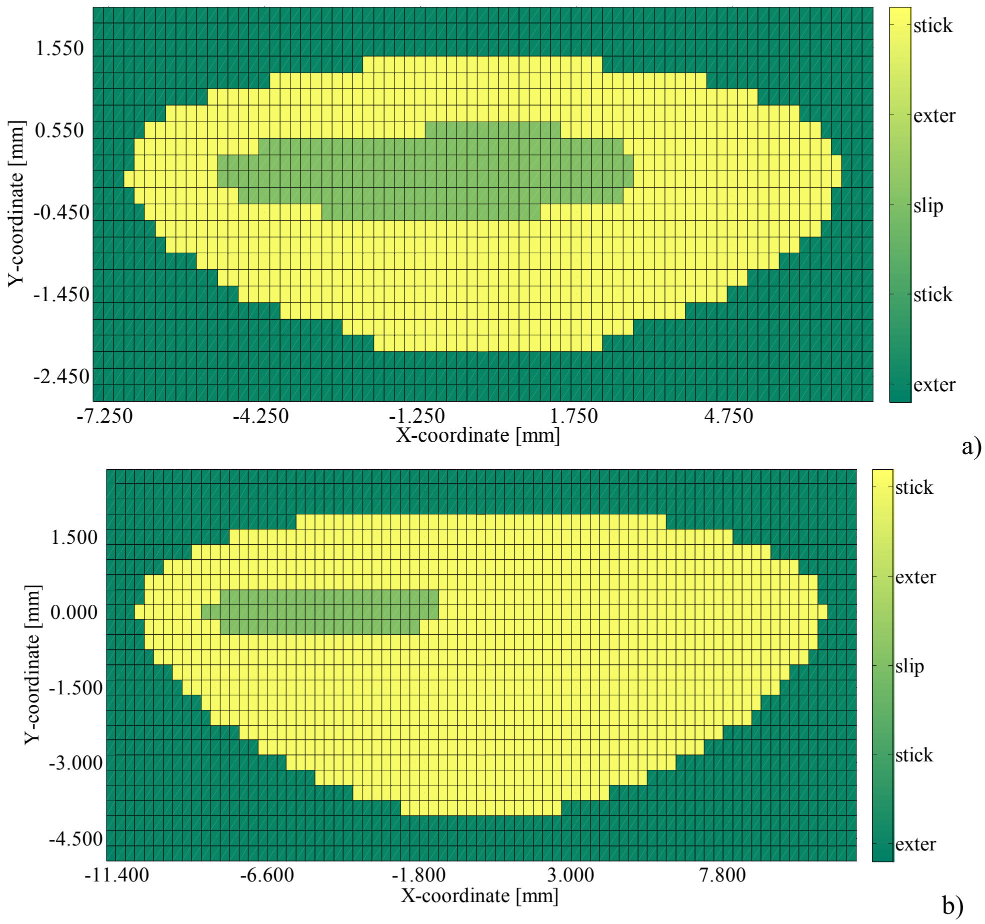

Fig. 3- The distribution of sliding and adherence areas in the case of a load shift over the first rolling wheel. a) – rolling on a railway with excess of super-elevation ; b) rolling on a railway with deficiency of super-elevation.

In fig. 4-a, b the distribution of the tangential traction force is presented. Taking into consideration that in the analysis a wheel with fray profile was introduced, for which the greater axis of the contact ellipse is orientated perpendicularly on the rail, one can observe that the tangential traction force intensifies towards the neck tor of the wheel edge.

This is explained by the fact that the guidance of the wheel is ensured by the edge of this when rolling on a track in both situations: with excess and with deficiency of super-elevation.

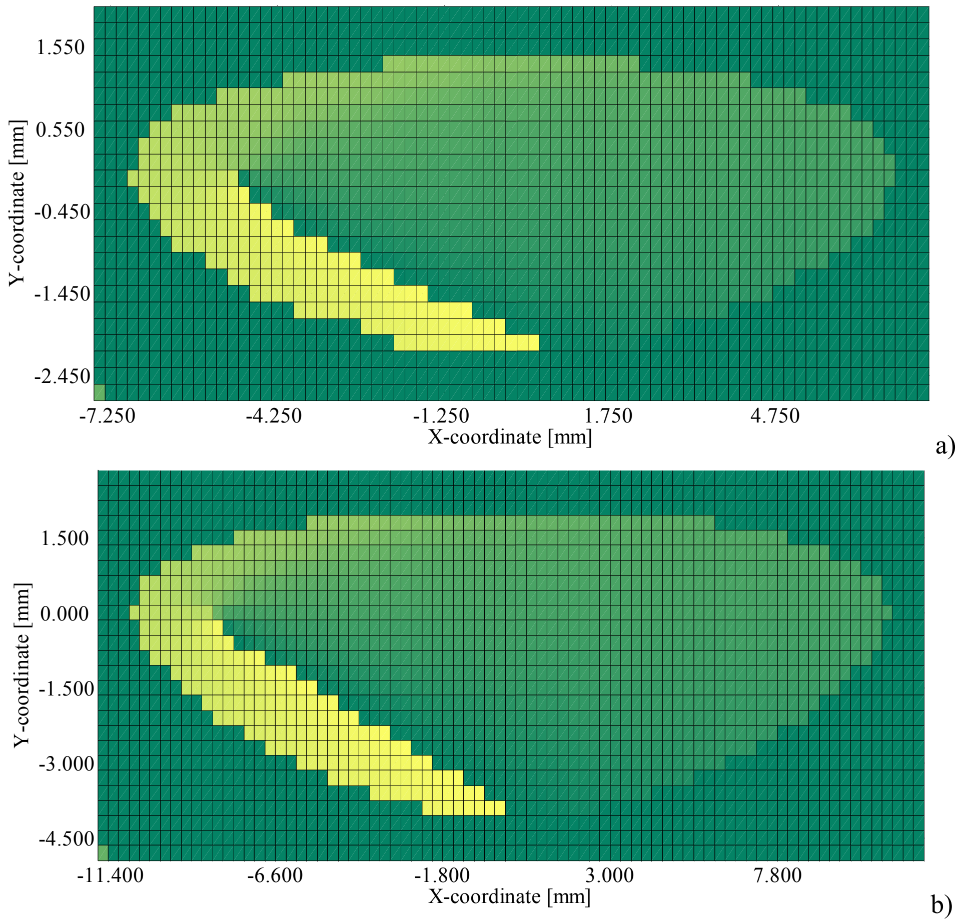

Fig. 4 - The distribution of the tangential traction force; a) – when rolling on a rail with excess of super-elevation; b) – when rolling on a rail with deficiency on super-elevation.

In figure number 5 the distribution of the friction power density from within the contact area is presented. The tribological aspect from within the contact area is strongly influenced by the load shift and by the state of the railway track. Thus a tribological build-up is observed in the contact area for the case when ravelling over an area with deficiency on super-elevation. This fact implies a tilt of the vehicle towards the exterior of the railway, which then leads to a transfer of load on the first rolling wheel; this explains the increase of the wear on the rolling surface of the wheel.

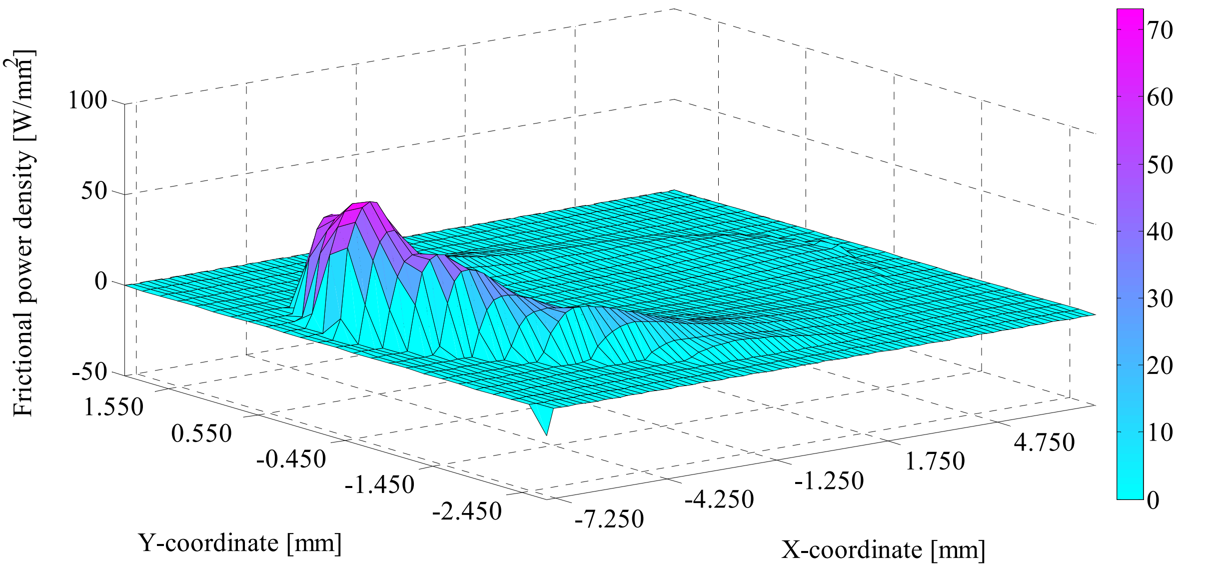

Fig. 5a - The distribution of the friction power; – rolling on a railway with excess of super-elevation

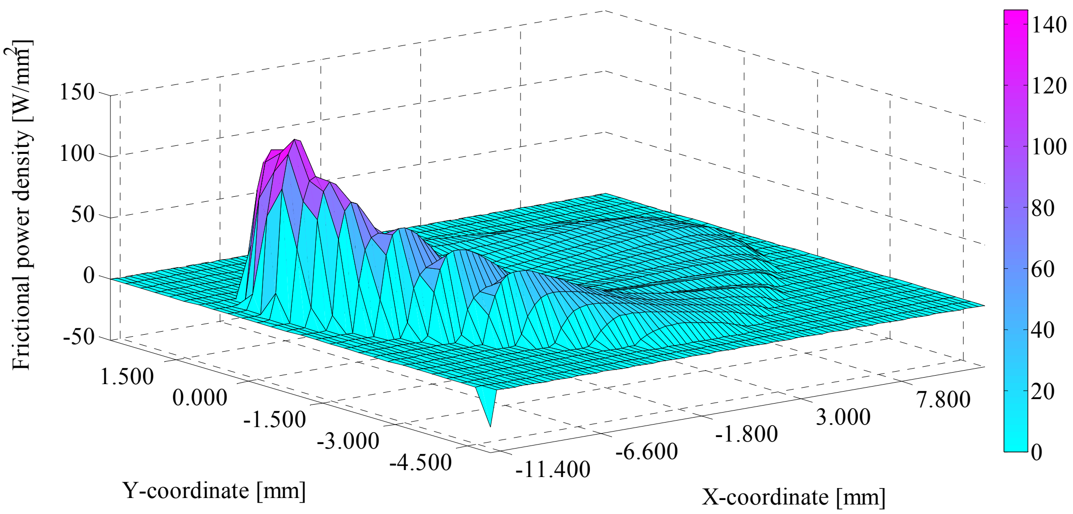

Fig. 5b - The distribution of the friction power; - rolling on a railway with deficiency on super-elevation

5. Conclusions

The present paper presents a tri-dimensional analysis method of the contact between the wheel and the railway. In this analysis Kalker's theory and Hertz's validity regarding simplifying hypotheses are taken into consideration, and are applied through the interactive CONTACT software.

The analysis set forth in the present paper validates the applicability of the CONTACT software for the profiles used by CFR (Romanian Railways). Also this approach leaves open the path for an evaluation from the tribological point of view of the vehicle behavior when rolling on a surface showing both excess and deficiency on super-elevation.

Finally, the analysis developed in the present paper ensures the knowledge of the phenomena, which occur in the contact area between the wheel and the railway and the effects they have on the safety of transportation.

Acknowledgment

The present paper was made within the framework of PN II PCCA tip 2, research contract ID 192/2012, financed by the Romanian Government through UEFISCDI.

Bibliography

[1]. Carter, F.W. (1926) *On the action of locomotive driving wheel*, in: Proc. Roy. Soc. A112, 151-7.
[2]. Johnson K. L. & Vermeulen, P. J. (1964) *Contact on non-spherical bodies transmitting tangential forces*, J. Appl. Mech., 31, (p. 338-340).
[3]. Haines D. J. & Ollerton, E. (1963) *Contact stress distribution on elliptical contact surfaces subjected to radial and tangential forces*, Proc. Inst. Mech. Eng. 177, (p.95-144).
[4]. Kalker, J. J. (1990) *Three-dimensional elastic bodies in rolling contact*, Dordrecht, Kluwer Academic Publishers.
[5]. Kalker, J. J. (2003) *Rolling contact phenomena*, Delft University of Technology, Netherlands,
[6]. Lévi, R. (1935) *Étude relative au contact des roues sur le rail*, Rev. Gen. Chem. Fer., 69, (p. 57-63), (in Franch).
[7]. Sebeşan, I. (2011) *Dinamica vehiculelor feroviare*, Editura MatrixRom, 2011.
[8]. Nadal, M. J. (1896) *Théorie de la stabilité des locomotives*, Mouvement de lacet. Ann. Mines Part II 10, (p. 232–255).
[9]. Weinstock, H. (1984) *Wheel climb derailment criteria for evaluation of rail vehicle safety*, Proceedings of the American Society of Mechanical Engineers Winter Annual Meeting, New Orleans (LA), 84–WA/RT–1: 1–7.
[10]. Jin, X., Ling L, Xiao X, Zhu M, Zhou Z. (2011) *Dynamic behavior numerical simulation and safety boundary analysis for high speed trains in severe environments*. Computer Aided Eng. 20 (3):29–41. Chinese.
[11]. Miyamoto, M, (1996) *Mechanism of derailment phenomena of railway vehicles*. QR RTRI. 37, (3):147–155.
[12]. Zhai, W. M., Chen, G. (2001) *Method and criteria for evaluation of wheel derailment based on wheel vertical rise*. Journal of the China Railway Society, 23(2):17–26, (in Chinese).
[13]. Vollebregt, E.A.H. (2012) *User guide for CONTACT, Vollebregt & Kalker's rolling and sliding contact model*, Technical Raport, VORtech computing, Delft, The Netherlands.
[14]. Tudorache, M. C. (2013) *The influence of wheel-rail phenomena upon guiding safety for railway vehicle*, PhD Thesis, Bucharest.
[15]. Deeg, E. W. (1992) *New Algorithms for Calculating Hertzian Stresses, Deformations, and Contact Zone Parameters*, AMP Journal of Technology Vol. 2.
[16]. Kalker, J. J. (1991) *Wheel-rail rolling contact theory*, wear 144, pp. 243-261.
[17]. Kalker, J. J. (1967) *A strip theory for rolling with slip and spin* , Proc. Kon. Ned. Akad. Van Wetenschappern, B70,10, 261-263.